

# Radiogenic Neutron Background v2.0

J. Cooley,<sup>3</sup> D.-M. Mei,<sup>4</sup> K.J. Palladino,<sup>2</sup> H. Qiu,<sup>3</sup> M. Selvi,<sup>1</sup> S. Scorza,<sup>3,5</sup> C. Zhang,<sup>4</sup> and ....

(The AARM Collaboration)

<sup>1</sup>*INFN - Sezione di Bologna, Italy*

<sup>2</sup>*Department of Physics, University of Wisconsin-Madison, Madison, WI 53706, USA*

<sup>3</sup>*Department of Physics, Southern Methodist University, Dallas, TX 75275, USA*

<sup>4</sup>*Department of Physics, University of South Dakota, Vermillion, USA*

<sup>5</sup>*Karlsruhe Institute of Technology, Institute of Experimental Nuclear Physics, Gaedestr. 1, 76128 Karlsruhe, Germany*

(Dated: January 21, 2016)

Ultra-low-background experiments, generically termed rare-event searches, address some of the most important open questions in particle physics, cosmology and astrophysics: direct detection of dark matter, neutrinoless double beta decay, proton decay, and detection of solar and supernovae neutrinos. Although their detection methods and physics goals are varied, rare-event searches share a number of common requirements in order to obtain sensitivity to low-rate processes in the presence of an overwhelming rate of environmental radiation, including the need for significant rock overburdens to moderate the flux of cosmic-ray muons. This requirement is so generic that an international community of underground science has emerged, with dozens of experiments operating in mines that vary in depth from a few hundred meters water equivalent (m.w.e.) to many thousand.

Simulations are used to understand backgrounds caused by naturally occurring radioactivity in the rock and in every piece of shielding and detector material used in the experiment. Most important are processes like spontaneous fission and  $(\alpha, n)$  reactions in material close to the detectors that can produce neutrons. A comparison study between two dedicated softwares is detailed. Neutron yields and spectra obtained with Mei-Zhang-Hime and SOURCES4 codes are presented.

## I. INTRODUCTION

Reduction of radiogenic backgrounds is one of the most important factors for rare event search experiments including searches for dark matter and neutrino-less double beta decay. These radiogenic backgrounds can be generically classified into two types: electron recoil and nuclear recoil backgrounds. Electron recoil background result from the interactions of gamma rays, electrons or beta particles interacting with the electrons in the detector's target medium while nuclear recoil backgrounds result from neutrons interacting with the nucleus in the detector's target medium. In dark matter experiments, the nuclear recoil background is of particular concern because a nuclear recoil from a neutron can be indistinguishable from a nuclear recoil from a WIMP.

Neutrons are produced by spontaneous fission,  $\alpha$ -n interactions and muon-induced interactions. Muon-induced neutrons can be reduced by operation the detector deep underground and by placing passive shielding around the detector. In addition, muon-induced neutrons can often be recognized by identifying the parent muon in a muon veto. More difficult to deal with are neutrons resulting from  $\alpha$ -n interactions and spontaneous fission from  $^{238}\text{U}$ ,  $^{235}\text{U}$ , and  $^{232}\text{Th}$  present in the materials the shielding and the detectors themselves. Thus, experimentalists must select their materials carefully when designing and constructing their experiments. This requires that they have accurate simulations of the processes in the materials they are considering.

There are currently two codes available for use in such calculations, SOURCES-4 and a second code developed

by Mei, Zhang and Hei which we will refer to as the USD code.

## II. NEUTRON YIELD AND SPECTRA

The measurements of neutron spectra strongly depend on the material and are not straightforward since neutrons are neutral particles. Their calculations is critical to low background experiments such as direct dark matter search experiments. The total neutron yield indicates the number of neutrons which are produced or had entered the target whereas the neutron energy spectrum determines the background events we would expect in the energy range of interest. Both are then needed in order to carry out a complete and reliable neutron background simulation. The evaluation of neutron yields and spectra can be performed via different codes: the modified version of SOURCES4A [1] and the code developed by Mei, Zhang and Hime [2] made available online at <http://neutronyield.usd.edu> have been considered. SOURCES4 code has been modified to extend the cross section for  $(\alpha, n)$  up to 10 MeV, based on experimental data, whenever possible, and calculations performed via the EMPIRE code [3] by the group at the University of Sheffield. SOURCES4A and USD codes calculate neutron yields and spectra from  $(\alpha, n)$  reactions due to the decay of radionuclides. Radiogenic neutrons are due to intrinsic contamination of materials surrounding the detectors of  $^{232}\text{Th}$ ,  $^{238}\text{U}$  and  $^{235}\text{U}$  decay chains. Comparison study between SOURCES4 and USD codes is carried out considering  $^{232}\text{Th}$ ,  $^{238}\text{U}$  decay chains in secular

equilibrium, although a possibility of disequilibrium can be taken into account: due to migration differently, the long-lived isotopes,  $^{226}\text{Ra}$ ,  $^{222}\text{Rn}$ ,  $^{210}\text{Po}$ ,  $^{228}\text{Ra}$ ,  $^{228}\text{Th}$  and the associated decay daughters could be calculated separately, see table I. For both chains, most of the neutrons are produced by the  $\alpha$  generated in the second part of the chains.

TABLE I. Radiogenic neutron yield ( $\text{n}\cdot\text{s}^{-1}\cdot\text{cm}^{-3}$ ) from  $(\alpha, \text{n})$  reactions in different materials for 1ppb of  $^{238}\text{U}$  and  $^{232}\text{Th}$  decay chains. Neutron yield have been calculated via the modified SOURCES4A code.

Material	Neutron yield for 1ppb ( $\text{n}\cdot\text{s}^{-1}\cdot\text{cm}^{-3}$ )	
	$^{238}\text{U} \rightarrow ^{226}\text{Ra}$	$^{226}\text{Ra} \rightarrow ^{206}\text{Pb}$
Stainless Steel	$6.4 \cdot 10^{-15}$	$3.1 \cdot 10^{-11}$
Pyrex	$4.0 \cdot 10^{-11}$	$1.9 \cdot 10^{-10}$
Borosilicate Glass	$6.3 \cdot 10^{-11}$	$2.8 \cdot 10^{-10}$
Titanium	$1.14 \cdot 10^{-13}$	$1.0 \cdot 10^{-10}$
Copper	$0.0 \cdot 10^{-11}$	$2.8 \cdot 10^{-12}$
PE ( $\text{C}_2\text{H}_4$ )	$1.6 \cdot 10^{-12}$	$1.1 \cdot 10^{-11}$
PTFE ( $\text{CF}_2$ )	$1.8 \cdot 10^{-10}$	$1.6 \cdot 10^{-9}$
Material	Neutron yield for 1ppb ( $\text{n}\cdot\text{s}^{-1}\cdot\text{cm}^{-3}$ )	
	$^{232}\text{Th} \rightarrow ^{228}\text{Th}$	$^{228}\text{Th} \rightarrow ^{208}\text{Pb}$
Stainless Steel	$8.8 \cdot 10^{-19}$	$4.1 \cdot 10^{-11}$
Pyrex	$2.4 \cdot 10^{-12}$	$8.4 \cdot 10^{-11}$
Borosilicate Glass	$3.8 \cdot 10^{-12}$	$1.2 \cdot 10^{-10}$
Titanium	$4.4 \cdot 10^{-16}$	$9.3 \cdot 10^{-11}$
Copper	$0.0 \cdot 10^{-11}$	$9.5 \cdot 10^{-12}$
PE ( $\text{C}_2\text{H}_4$ )	$1.6 \cdot 10^{-13}$	$5.1 \cdot 10^{-12}$
PTFE ( $\text{CF}_2$ )	$7.1 \cdot 10^{-12}$	$7.7 \cdot 10^{-10}$

The calculation of the neutron spectra requires as input the cross-sections of  $(\alpha, \text{n})$  reactions, the probabilities of nuclear transition to different excited states (branching ratio) and the alpha emission lines from the radioactive radionuclides. Both codes consider a thick target: calculation of neutron yields and spectra are carried out under the assumption that the size of radioactive sample exceeds significantly the range of alpha. The energy bin size of the  $(\alpha, \text{n})$  calculation is fixed to be 0.1 MeV in USD code while is user dependent in SOURCES4A.

Table II lists  $\alpha$ -lines respectively for  $^{232}\text{Th}$  and  $^{238}\text{U}$  decay chains, present in SOURCES4A and USD codes. USD code is missing the lines coming from  $^{222}\text{Ra}$  isotope in  $^{238}\text{U}$  decay chain which SOURCES4A library is considering. Overall, the branching ratio and the energy lines are in good agreement between the two codes.

Cross-sections and branching ratios are required as well for neutron yield and spectra calculations. The USD code considers TENDL 2012 [4] to provide  $(\alpha, \text{n})$  nuclear cross-sections. TENDL is a validated nuclear data library which provides the output of the TALYS [5] nuclear model code system; SOURCES4 cross section input libraries come from EMPIRE2.19 [3] calculations and, for some isotopes, a combination of data measurements and EMPIRE2.19 calculations. Also, EMPIRE is the code recommended by International Atomic Energy Agency (IAEA). Neither EMPIRE nor TALYS can calculate properly resonance behavior which has been ex-

TABLE II. Alpha lines present in SOURCES4A and USD, and their intensity (BR) for isotopes in the  $^{232}\text{Th}$  and  $^{238}\text{U}$  decay chains. Only lines with intensity  $> 1\%$  have been quoted.

SOURCES4A			USD	
Isotopes	Line (keV)	BR (%)	Line (MeV)	BR (%)
$^{238}\text{U}$	4151	21	4.151	21
	4198	79	4.198	79
$^{234}\text{U}$	4722.4	28.42	4.722	28.6
	4774.6	71.38	4.775	71.4
$^{230}\text{Th}$	4620.5	23.4	4.621	23.7
	4687.0	76.3	4.688	76.3
$^{226}\text{Ra}$	4601	5.55	4.602	5.6
	4784.34	94.45	4.784	94.4
$^{222}\text{Rn}$	5489	99.92	5.490	100
$^{218}\text{Po}$	6002.35	99.98	6.002	100
$^{214}\text{Po}$	7686.82	99.99	7.687	99.99
$^{210}\text{Po}$	5304.33	99.99	5.304	100
$^{232}\text{Th}$	3947.2	21.7	3.954	22.1
	4012.3	78.2	4.013	77.9
$^{228}\text{Th}$	5340.36	27.2	5.340	28.5
	5423.15	72.2	5.423	71.5
$^{224}\text{Ra}$	5448.6	5.06	5.449	5.1
	5685.37	94.92	5.685	94.9
$^{220}\text{Rn}$	6288.3	99.99	6.288	100
$^{216}\text{Po}$	6778.5	99.99	6.778	100
$^{212}\text{Bi}$	6051.1	25.16	6.050	26.2
	6090.2	9.79	6.0902	9.8
$^{212}\text{Po}$	8784.6	100	8.784	64

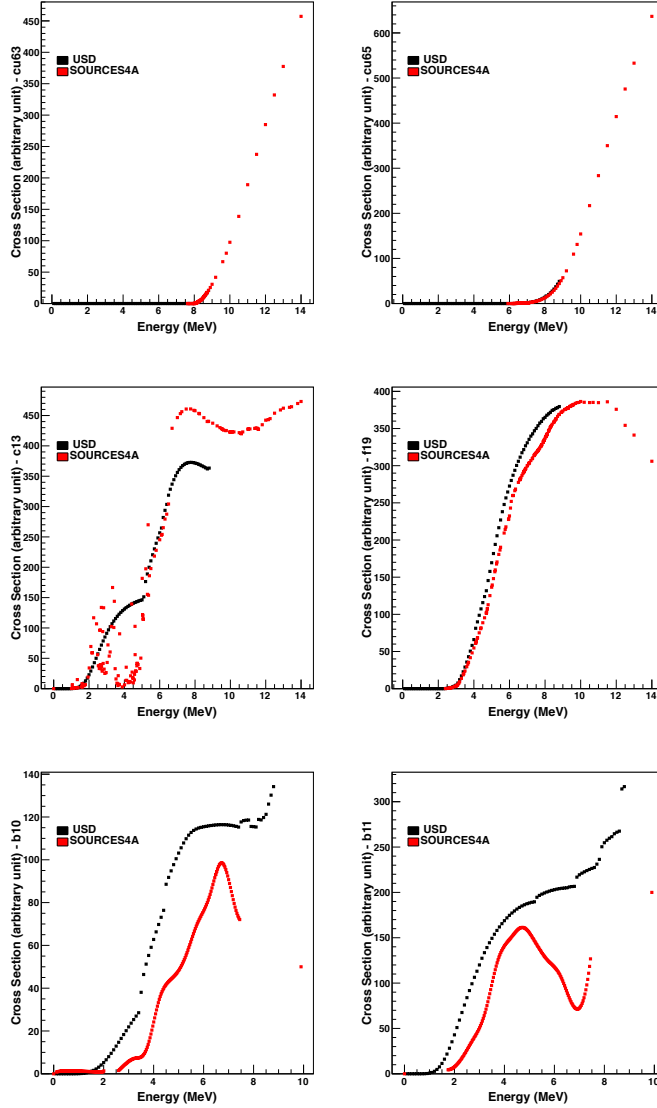
TABLE III. Radiogenic neutron yield ( $\text{n}/\text{s}/\text{cm}^3$ ) for copper and polyethylene materials and for  $^{238}\text{U}$  and  $^{232}\text{Th}$  decay chains. Column (1) and (2) refer to pure USD and SOURCES4A calculation, respectively. Column (3) refers to SOURCES4A calculation with USD  $(\alpha, \text{n})$  cross section libraries. A ratio of the neutron yield is also provided: column (a) refers to the ratio of (2) over (1), whereas column (b) corresponds to the ratio (2)/(3).

Material	Chain	Neutron Yield ( $10^{-12} \cdot \text{n}\cdot\text{s}^{-1}\cdot\text{cm}^{-3}$ )			Ratio	
		(1)	(2)	(3)	(a)	(b)
Copper	$^{238}\text{U}$	3.46	2.84	2.93	0.8	1.0
	$^{232}\text{Th}$	11.1	9.49	9.18	0.9	1.0
Polyethylene ( $\text{C}_2\text{H}_4$ )	$^{238}\text{U}$	9.56	12.6	16.4	1.3	0.8
	$^{232}\text{Th}$	2.87	5.28	5.97	1.8	0.9

perimentally observed.

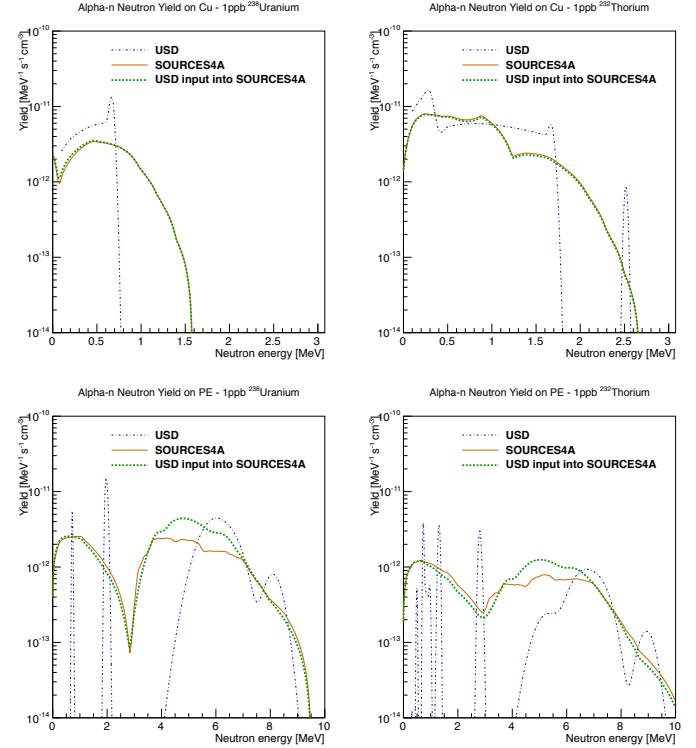
An extensive comparison between the different cross-section libraries used in USD and SOURCES4A has been carried out for the target nuclides present in the materials contributing the most to radiogenic neutron background. Specifically, we refer to materials which compose the shielding scheme and the internal detector parts, such as stainless steel, copper, titanium, borosilicate glass (PMTs glass), PTFE which become important when the external flux is attenuated by the shielding. Comparison of cross section inputs results in a good agreement for most of isotopes in both code libraries. For some,

FIG. 1. Input ( $\alpha, n$ ) cross-section for the target isotopes involved in radiogenic neutron calculations for copper and polyethylene. Red markers refers to SOURCES4A inputs, whereas the black markers to USD. From left to right, top to bottom:  $^{63}\text{Cu}$ ,  $^{65}\text{Cu}$ ,  $^{13}\text{C}$ ,  $^{19}\text{F}$ ,  $^{10}\text{B}$  and  $^{11}\text{B}$ .



such as  $^{13}\text{C}$  and  $^{10}\text{B}$  and  $^{11}\text{B}$  the cross sections show discrepancies. To better understand the contribution due to the cross section input library in the radiogenic neutron yield and spectrum we have calculated radiogenic neutron yield and spectra for two different materials: copper, for which the input cross sections in both codes are matching, and polyethylene, for which input cross sections of  $^{13}\text{C}$  show discrepancies between the codes, details in figure 1. We have considered natural copper (70%  $^{63}\text{Cu}$  and 30%  $^{65}\text{Cu}$ ) with a density of  $8.96 \text{ g/cm}^3$ ; polyethylene material ( $\text{C}_2\text{H}_4$ ) is considered with a density of density is  $0.935 \text{ g/cm}^3$ . Estimates are done for 1ppb

FIG. 2. Radiogenic neutron spectra ( $\text{n}\cdot\text{MeV}^{-1}\cdot\text{s}^{-1}\cdot\text{cm}^{-3}$ ) calculated for 1ppb  $^{238}\text{U}$  and  $^{232}\text{Th}$  decay chains, left and right panels, respectively. First row show copper contribution, lower row polyethylene material. Dotted blu lines refers to pure USD calculations, plain orange line to pure SOURCES4A calculations and dashed green line is the mixed computation for which we ran SOURCES4A algorithm with input cross section of USD code.



in  $^{238}\text{U}$  and  $^{232}\text{Th}$  decay chains. Calculations consist of pure SOURCES4A and USD computation and a mixed computation for which we run SOURCES4A algorithm with cross section inputs of USD. Resulting radiogenic neutron yields are quoted in table III. The column (a) of the radiogenic neutron yield ratio quotes the calculation differences between SOURCES4A and USD codes: they show a reasonably good agreement, inside a 50% discrepancy. The column (b) refers to the ratio of radiogenic neutron yield resulting from the same algorithm calculation (SOURCES4A) but with USD (column (3)) and SOURCES4A (column (2)) input ( $\alpha, n$ ) cross-sections. For polyethylene, we can conclude that the input cross-section may account up to a 20% discrepancy in neutron yield. Figure 3 shows radiogenic neutron spectra for copper (upper row) and polyethylene (lower row), both from uranium and thorium decay chains, left and right panels respectively.

A comparison of neutron yield and energy spectrum obtained via SOURCES4A and USD codes for different material has been carried out. Results are shown in table IV and figure 3. A qualitative agreement between

the two codes is observed. A maximum discrepancy of a factor 2 is found. The energy spectra calculated via SOURCES4A code are in general smoother, without the presence of peaks, feature of USD spectra.

TABLE IV. Radiogenic neutron yield ( $\text{n}\cdot\text{s}^{-1}\cdot\text{cm}^{-3}$ ) per material considering 1ppb of  $^{238}\text{U}$  and  $^{232}\text{Th}$ . The percentage difference is calculated as  $(\text{SOURCES4A}-\text{USD})/[(\text{SOURCES4A}+\text{USD})/2]$ .

Material	Chain	Neutron Yield ( $\text{n}\cdot\text{s}^{-1}\cdot\text{cm}^{-3}$ )		Diff %
		SOURCES4A	USD	
Cu	$^{238}\text{U}$	2.84E-12	3.46E-12	20
	$^{232}\text{Th}$	9.49E-12	1.11E-11	16
PE ( $\text{CH}_2$ )	$^{238}\text{U}$	1.26E-11	9.56E-12	-27
	$^{232}\text{Th}$	5.28E-12	2.87E-12	-59
Titanium	$^{238}\text{U}$	$1.04 \cdot 10^{-10}$	$1.99 \cdot 10^{-10}$	-63
	$^{232}\text{Th}$	$9.29 \cdot 10^{-11}$	$1.24 \cdot 10^{-10}$	-28
Stainless Steel	$^{238}\text{U}$	$3.10 \cdot 10^{-11}$	$5.95 \cdot 10^{-11}$	-63
	$^{232}\text{Th}$	$4.05 \cdot 10^{-11}$	$6.80 \cdot 10^{-11}$	-51
Pyrex	$^{238}\text{U}$	$2.30 \cdot 10^{-10}$	$1.61 \cdot 10^{-10}$	36
	$^{232}\text{Th}$	$8.66 \cdot 10^{-11}$	$4.59 \cdot 10^{-11}$	61
Borosilicate Glass	$^{238}\text{U}$	$3.48 \cdot 10^{-10}$	$2.45 \cdot 10^{-10}$	35
	$^{232}\text{Th}$	$1.27 \cdot 10^{-10}$	$6.98 \cdot 10^{-11}$	58
PTFE ( $\text{CF}_2$ )	$^{238}\text{U}$	$1.81 \cdot 10^{-9}$	$1.60 \cdot 10^{-9}$	12
	$^{232}\text{Th}$	$7.76 \cdot 10^{-10}$	$5.42 \cdot 10^{-10}$	36

### III. GEANT4 PROPAGATION

To evaluate the impact of the varying neutron spectra produced by SOURCES4A and the USD calculator, simplified detector geometries were created within a RAT [6] framework with Geant4.9.5.p01 and the pertinent high precision neutron physics list utilizing cross sections from G4NDL3.14 for neutrons under 20 MeV. Four simulations, for neutrons from uranium and thorium, with the spectra from SOURCES4A and USD (shown in Figure /reffig:ratspectra) were run for each relevant material under study.

Three simplified direct dark matter detector geometries were established to study neutron elastic scatter signals within central detector materials and the potential for vetoing neutrons with outer detectors. The first was a spherical liquid argon detector, with a radius of 1 m, is surrounded by shells of 10 cm thick acrylic, 5 mm thick borosilicate glass, and a water veto out to a radius of 3 m. The simulated neutrons were isotropically created in the borosilicate glass, as it is the leading source of radiogenic neutrons in many liquid argon detectors.

The second geometry studied was a cylindrical liquid xenon detector with a 1 m diameter and height. It is nested within cylinders of 3 cm thick PTFE, 2 cm thick titanium, and liquid scintillator veto with a diameter and height of 3 m. Neutrons were generated isotropically in

the PTFE for variety of materials studied; it is not likely to be the leading source of neutron backgrounds for most xenon detectors.

The final geometry studied was a cylindrical solid germanium detector with a 10 cm diameter and 120 cm height. It is surrounded by nested cylinders: first 1 cm thick copper, then 15 cm of polyethylene veto and 10 cm of lead. The neutrons are generated isotropically within the copper.

For these sample studies, an analysis threshold on the neutron-induced nuclear recoils of 20 keV was set in the argon detector and 5 keV in the xenon and germanium detectors. Scatters were rejected as WIMP-like recoils if there were multiple nuclear scatters over threshold within the target. Figure /reffig:nuclearrecoils shows the induced nuclear recoil spectra in these simulated detector targets along with the single nuclear recoil spectra. The larger liquid noble detectors show greater reductions from all nuclear scatters to single nuclear scatters due to their size. The induced recoil spectra visibly smooth out the neutron spectra, and the differences between simulations originating with the SOURCES4A and USD are minimized when studying the single nuclear recoils of interest.

TABLE V. The differences in nuclear recoil counts over threshold simulated for different origin and target materials with SOURCES 4A and USD initial neutron spectra and yields. The percentage difference is calculated as  $(\text{SOURCES4A}-\text{USD})/[(\text{SOURCES4A}+\text{USD})/2]$ . The  $\chi^2$  per degree of freedom is calculated just for the single recoil spectra shape and excludes the normalization to total neutron yield.

Materia/Target	Chain	Recoils Diff%	Singles Diff%	$\chi^2/\text{NDF}$
Borosilicate/Ar	$^{238}\text{U}$	23	34	1.24
	$^{232}\text{Th}$	27	41	1.32
PTFE/Xe	$^{238}\text{U}$	-2	11	1.89
	$^{232}\text{Th}$	23	26	1.06
Cu/Ge	$^{238}\text{U}$	-81	-58	152
	$^{232}\text{Th}$	-16	-14	5.83

Table V provides the percentage difference between the simulated nuclear recoil counts from SOURCES4A and USD neutron spectra. The difference in counts for the borosilicate and PTFE studies can nearly all be attributed to the difference in the total neutron yields. Indeed, these count differences are generally smoothed out and reduced proportionately from the yield differences in Table IV, and a  $\chi^2$  per degree of freedom test of just the recoil spectra shapes shows reasonable agreement between both simulations.

This is not the case for the neutrons originating in copper. The total yields began with a 20% agreement, but the truncation in energy of the USD spectra causes a significant difference of up to 80% for the numbers of recoils seen above threshold. These differences are easily seen in the lower-left panel of Figure 4 for the  $^{238}\text{U}$

neutrons originating in Cu and recoiling in a Ge target. Additional tests, that are not shown here there, vetoed events with more than 1 keV deposited from inelastic or capture gamma ray scatters within the target, or if a neutron capture occurred within the veto material. Although no common dopants were included in the veto materials, most neutrons did capture within the vetoes. The remaining elastic nuclear scatters comparisons between SOURCES and USD initial spectra were analogous to those for the single recoils.

The impact upon neutron background simulations for dark matter detectors of the difference between ( $\alpha$ , n) neutron spectra calculated with SOURCES4A and the

USD webtool is primarily one of overall normalization. The differences would lead to different background predictions prior to running an experiment, but when spectral fits are made to recoils seen in a detector for multiple scatters, high energy or high radius events, the prediction of low energy single nuclear recoils is quite robust. However, there may be other exceptions besides copper to these spectral considerations.

RAT reference needs to be added

#### IV. CONCLUSION

- 
- [1] W. Wilson, R. Perry, W. Charlton, and T. Parish, Progress in Nuclear Energy **51**, 608 (2009).  
 [2] D. M. Mei, C. Zhang, and A. Hime, Nucl. Instrum. Meth. **A606**, 651 (2009), arXiv:0812.4307 [nucl-ex].  
 [3] E.-I. statistical model code for nuclear reaction calculation, <https://www-nds.iaea.org/empire218/manual.ps..>.  
 [4] A. Koning, D. Rochman, S. van der Marck, J. Kopecky, J. C. Sublet, S. Pomp, H. Sjostrand, R. Forrest, E. Bauge, and H. Henriksson, TENDL-2012: TALYS-based evaluated nuclear data library, <ftp://ftp.nrg.eu/pub/www/talys/tendl2012/tendl2012.html>.  
 [5] A. Koning and D. Rochman, Nuclear Research and Consultancy Group (NRG), <http://www.talys.eu/documentation/>.  
 [6] "Rat (is an analysis tool) users guide," <http://rat.readthedocs.org/en/latest/>, accessed: 2016-01-21.

FIG. 3. Radiogenic neutron spectra ( $\text{n} \cdot \text{MeV}^{-1} \cdot \text{s}^{-1} \cdot \text{cm}^{-3}$ ) calculated for 1ppb  $^{238}\text{U}$  and  $^{232}\text{Th}$  decay chains, left and right panels, respectively. The  $(\alpha, n)$  reaction contribution is shown in various commonly used materials from SOURCES4A in orange and USD in blue. From top to bottom materials are: copper, titanium, stainless steel, pyrex, borosilicate glass, polyethylene and teflon (PTFE).

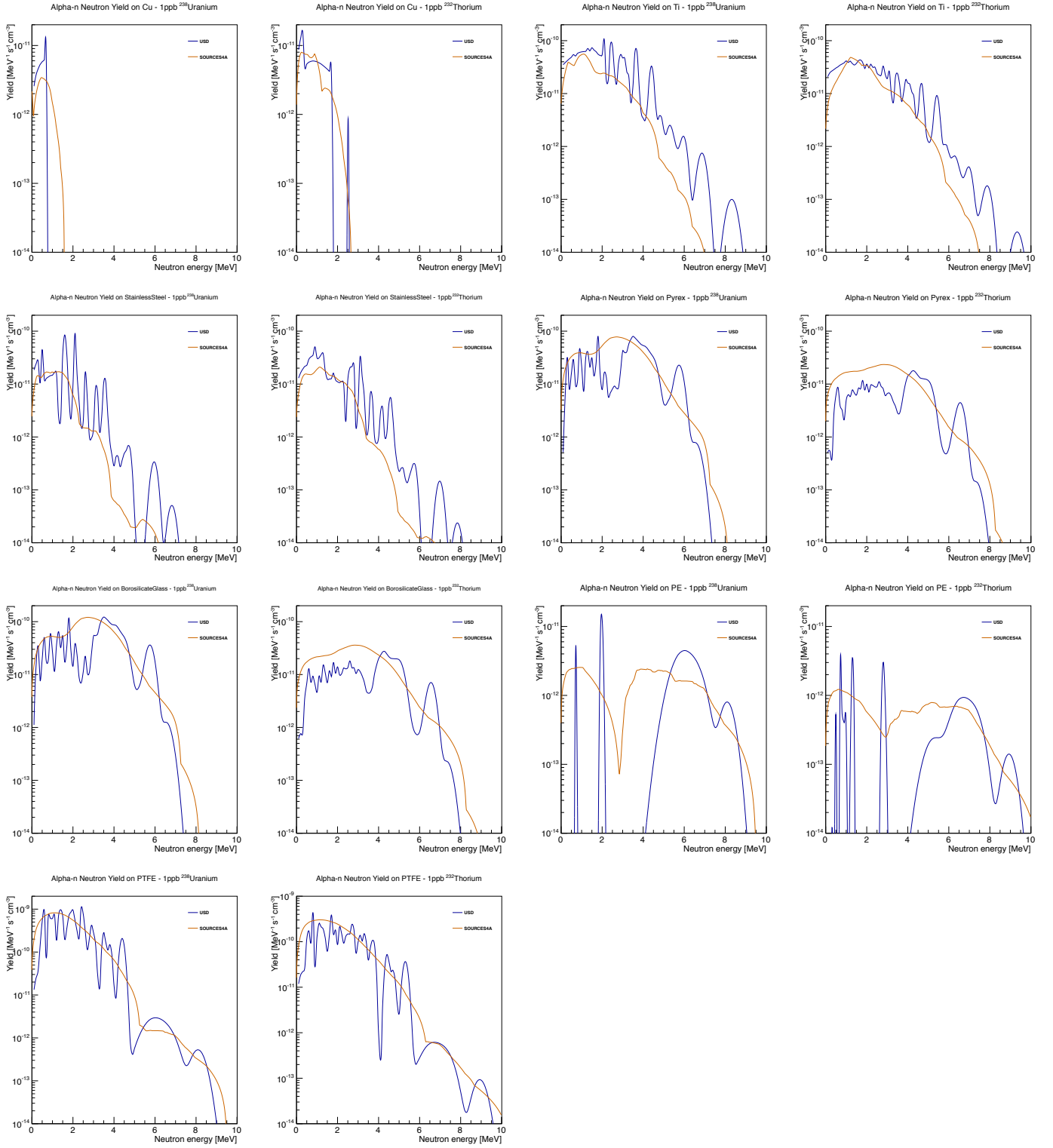


FIG. 4. Comparisons of nuclear recoils in simplified direct dark matter detector GEANT4 simulations induced from ( $\alpha$ , n) neutrons originating in detector materials. All red lines correspond to SOURCES4A initial spectra, while the USD initial spectra are plotted in blue. The solid lines are histograms of all individual nuclear recoils in the target materials, while the dashed lines are irreducible single nuclear recoils within the target. On the left are simulations for  $^{238}\text{U}$ , and  $^{232}\text{Th}$  spectra are on the right. The detectors from top to bottom are an argon target with neutrons originating in borosilicate glass, a xenon target with neutrons originating in PTFE, and a germanium target with neutrons originating in copper.

